Effects of Variation of Quantum Well Number on the Performance of a Designed 635nm $Ga_{0.5}In_{0.5}P/(Al_{0.7}Ga_{0.3})_{0.5}In_{0.5}P$ Multiple Quantum Well Red Laser

Tawsif Ibne Alam, Md. Abdur Rahim and Rinku Basak

***Abstract*– In this work, the effects of variation of the number of quantum well on the performance characteristics of a GaInP - based 635nm multiple quantum well (MQW) separate confinement heterostructure (SCH) Red laser have been obtained through computations. The peak material gain of $Ga_{0.5}In_{0.5}P/(Al_{0.5}Ga_{0.5})_{0.5}In_{0.5}P$ MQW edge emitting laser obtained from the analysis has been used for analyzing the performance characteristics of the designed laser. The number of QW is optimized as 3 for obtaining better performance characteristics where the threshold current of the designed device is 6.7 *mA*. A maximum output power of 71.18 *mW* , a maximum resonance frequency of 8.6 GHz and a maximum modulation bandwidth of 13.85 GHz have been obtained for this designed laser at 64 *mA* injection current at 300K temperature having a 3QW structure.**

***Keywords*– Laser Diode, Double-Heterostructure, EEL, QW and Red Laser**

I. INTRODUCTION

The development in the double-heterostructure was first implemented during the 1970s [1]. The recent refinements and their use in short wavelength lasers have found widespread application in communication, and medical science. Particular interest in the 635*nm* wavelength shows significant contribution to fiber optic communication, optical disk recording, medical science, (photo dynamic therapy) and other applications that led us to concentrate our interest on the performance analysis and optimization of this short wavelength laser.

Since their first demonstration during the 1985 [2] the only material system ever to support red emission wavelength was reported to be GaInP/AlGaInP. It has been reported that the carrier confinement in GaInP/AlGaInP quantum wells of the single heterostructure, especially the electron confinement, is very poor due to AlGaInP having a maximum allowable direct bandgap of only about 2.32 eV [2].

Tawsif Ibne Alam is a Graduate, Department of EEE, Faculty of Engineering, American International University-Bangladesh (AIUB), Banani, Dhaka-1213, Bangladesh. Email: treblz.89@gmail.com, treblz@hotmail.com

Md. Abdur Rahim is a Graduate, Department of EEE, Faculty of Engineering, American International University-Bangladesh (AIUB), Banani, Dhaka-1213, Bangladesh. Email: rahimabdur.2012@gmail.com

Rinku Basak is an Assistant Professor and Head (Graduate Program), Department of EEE, Faculty of Engineering, American International University-Bangladesh (AIUB), Banani, Dhaka-1213, Bangladesh. Email: rinku_biju@yahoo.com, rinku@aiub.edu

Theory of Quantum well lasers suggests that QW laser diodes have narrow active region for which quantum confinement occurs. The wavelength of the light emitted by a quantum well laser is determined by the width of the active region rather than just the bandgap of the material from which it is constructed. This means that much shorter wavelengths can be obtained from quantum well lasers than from conventional laser diodes using a particular semiconductor laser. The added advantage of the QW lasers is its efficiency. Quantum well lasers have greater efficiency than a conventional laser diode due to the stepwise form of its density of states function.

In this paper, the performance analysis and optimization of a 635*nm* $Ga_{0.5}In_{0.5}P/(Al_{0.5}Ga_{0.5})_{0.5}In_{0.5}P$ MQW Separate Confinement Heterostructure Red Laser are presented considering the effects of quantum well number variation.

II. THEORY

A. Energy sub-band

Energy levels in some of the sub-band in the quantum well region are developed above the conduction band edge while some are created below the valance band edge. The actual transitions take place between these conduction sub-bands to valence sub-bands. For both the conduction and valence sub-bands, the discrete energy levels in the quantum well region are found out using the time independent Schrodinger equation solution under effective mass approximations, because of parabolic nature of the bands [3]

$$\nabla^2\psi + \frac{\hbar^2}{2m_e}(E - V) = 0 \qquad (1)$$

where, ψ is the particle wave function, $\hbar$ is the Planck's constant divided by 2π, m_e is the effective mass of the carrier, V is band potential and E is the energy levels of the conduction band or the valence band.

B. Gain Calculation

For the active region material, the optical gain has to be obtained in order to design a practical laser. This is done by computing the gain at the operating wavelength, also within a fine range around it. The gain expression is given as [4], [5].

$$g(E) = \left(\frac{q^2\pi\hbar}{\varepsilon_0 m_0{}^2 n_r cE}\right)|M_T|^2\rho_r(f_2 - f_1) \qquad (2)$$

where, q is the electronic charge, ε_0 is the free space permittivity, c is the speed of light, n_r is the refractive index of the laser structure, E is the transition energy, $m_0$is the mass of electron, $|M_T|^2$ is the square of the transition momentum matrix element, ρ_r is the reduced density of state, $\hbar$ is the Planck's constant divided by 2π, f_2 and f_1 are quasi-Fermi functions in the conduction and valance band respectively.

III. STRUCTURE AND DESIGN OF THE 635*nm* RED LASER

A. Energy gap calculation and design of laser cavity

In this work, for achieving high performance, the Ga, In and P concentration of GaInP QW material is chosen from the results obtained after computation using Vegard's law [6]. The results are found to coincide with other research works. For the $Ga_{0.5}In_{0.5}P$ quantum wells, higher material peak gain near the emission wavelength of 635*nm* and lower transparency carrier density is achieved, for which it has been used in this design. The active region consists of three quantum wells, each having a thickness of 80Å which are separated by $(Al_{0.5}Ga_{0.5})_{0.5}In_{0.5}P$ barriers of thickness 100Å.

At 300 K, the bandgap energies of the $Ga_{0.5}In_{0.5}P$ material in the quantum well region, $(Al_{0.5}Ga_{0.5})_{0.5}In_{0.5}P$ material in the barrier and SCH region are obtained with the well known equations [7] and shown in Fig. 1.

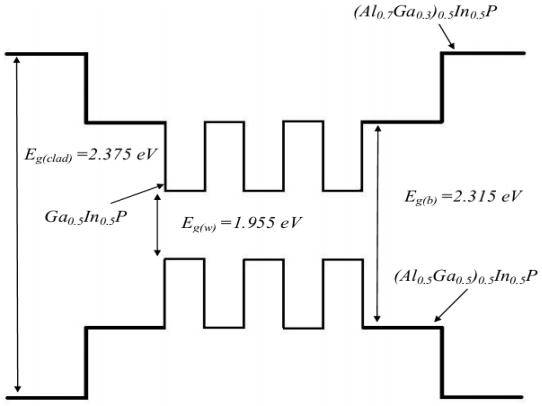

Fig. 1. The active region of a SCH Red Laser consisting 3 quantum wells of 80Å each

Fig. 1. shows the bandgap energy of the cavity of the designed laser. The active region is sandwiched by a SCH layer of $(Al_{0.5}Ga_{0.5})_{0.5}In_{0.5}P$ having a thickness of 900Å each and are enclosed within a cladding layer of $(Al_{0.7}Ga_{0.3})_{0.5}In_{0.5}P$ which has been doped. The ends of the device are cleaved to form flat planes called 'facets' that act as partially reflective mirrors allowing an achievement of reflectivity of 33.5%. Current is injected through the upper p-type contact of the device and the lower n-type contact is placed at the bottom of the GaAs substrate as shown in Fig. 2.

B. Calculation of Material Gain

Theoretically, for designing an edge emitting Red laser, an optimum choice of material gain and transparency carrier density of $Ga_{0.5}In_{0.5}P$ material have to be obtained. The transparency carrier density of a material is related to the effective masses of carriers in the conduction band (CB) and valance band (VB) as [4], [5].

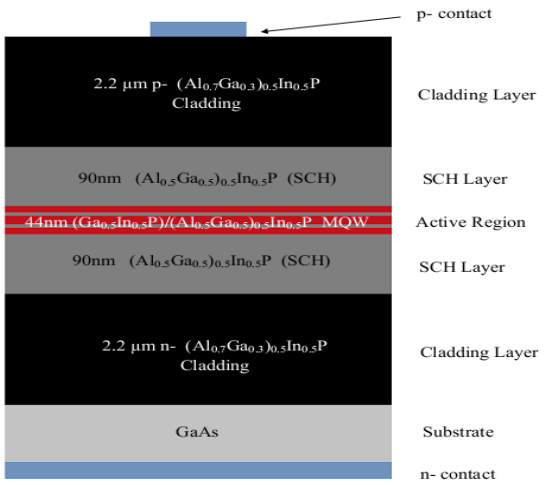

Fig. 2. The structure of a designed 635nm MQW Red Laser

$$N_{tr} = 2\left(\frac{kT}{2\pi\hbar^2}\right)^{3/2}(m_c m_v)^{3/4} \qquad (3)$$

where, k is the Boltzmann constant, T is the temperature in K, $\hbar$ is the Planck's constant divided by 2π, $m_c$and m_v are the effective masses of the carriers in the CB and VB respectively. This relationship is used to compute the transparency carrier density of QW material.

At 300 K, the calculated value of transparency carrier density for $Ga_{0.5}In_{0.5}P$ is $1.1513 \times 10^{18}\ cm^{-3}$. This value is lower than that of the barrier material for which it is suitable to use as the QW material.

Using equation (2), at 300K the material gain for a 635*nm* $Ga_{0.5}In_{0.5}P/(Al_{0.5}Ga_{0.5})_{0.5}In_{0.5}P$ 80Å MQW SCH Red Laser is calculated by varying wavelength. It is essential to arrange so that the cavity oscillation occurs at the peak value of the gain of the material. The obtained results are plotted as shown in Fig. 3. A peak material gain value of $766.6\ cm^{-1}$ is obtained for the $Ga_{0.5}In_{0.5}P/(Al_{0.5}Ga_{0.5})_{0.5}In_{0.5}P$ MQW SCH EEL around the wavelength of 610 nm.

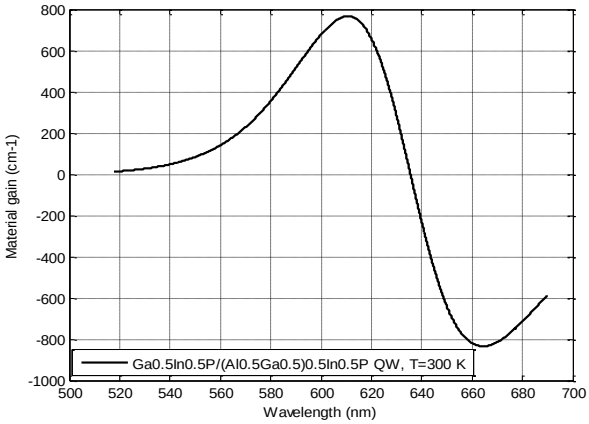

Fig. 3. Plot of material gain vs. wavelength of the designed $Ga_{0.5}In_{0.5}P/(Al_{0.5}Ga_{0.5})_{0.5}In_{0.5}P$ 3QW SCH edge emitting Red laser at 300K. The material gain of the designed laser varies with the variation of wavelength and a maximum gain is obtained as $766.6\ cm^{-1}$ at 610*nm* wavelength.

Using the obtained value of the peak material gain the performance characteristics of the designed 635*nm* SCH edge emitting Red laser have been presented in the following section.

IV. PERFORMANCE CHARECTRISTICS OF THE DESIGNED SCH EEL

A. Key Parameters of the designed laser

The key parameters of the designed laser have been presented below. Some of the parameters are also included in this list from practically implemented lasers from the following sources [6], [8].

Table I. Parameter Values of The Designed Laser

Type of Parameters	Value
Active Region Volume (V)	$7.92 \times 10^{-11}\ cm^3$
Cavity Volume (V_p)	$4.032 \times 10^{-10}\ cm^3$
Confinement factor (Γ)	0.1964
Electron effective mass (m_e)	$0.092m_0$
Hole effective mass (m_h)	$0.179m_0$
Temperature in Kelvin	300K
Differential gain (a)	$5.1 \times 10^{-16}\ cm^2$
Injection current (I)	64 *mA*
Intrinsic absorption loss (α_i)	$5\ cm^{-1}$
Reflectivity (R)	0.335
Gain compression factor (ε)	$1.5 \times 10^{-17}\ cm^3$
Spontaneous emission factor (β_{sp})	0.869×10^{-4}
Spontaneous emission rate (R_{sp})	1×10^3

B. Computation of threshold carrier density N_{th}, photon life time τ_p and threshold current I_{th} of the designed laser

At 300K, the threshold carrier density of $1.2902 \times 10^{18}\ cm^{-3}$has been found out using the well known expression [5]. With the threshold carrier density found out, the photon lifetime is then obtained using the well known expression [5] as $6.637\ ps$ from a group velocity v_g of $8.7848 \times 10^9\ cms^{-1}$.

The threshold current is then calculated using the following expression [5].

$$I_{th} = \frac{q \times V \times N_{th}}{\eta_i \times \tau_c} \qquad (4)$$

where, η_i is the injection current efficiency, N_{th} is the threshold carrier density and τ_c is the carrier life time in the conduction band.

It is found that at 300K the threshold current is as small as 6.7 *mA* with an injection current efficiency (η_i) of 0.9.

C. *Computation of the Performance Characteristics and Results*

The solution to the rate equations [5], [9] have been obtained using the parameter values, for a time window of 0-3*ns* approximately using finite difference method in MATLAB for a chosen (applicable) value of injection current of 64 *mA*. The value of injection current is to be taken so that it is above threshold current. A plot of carrier density vs. time is shown in fig.4 for the designed 635*nm* red laser.

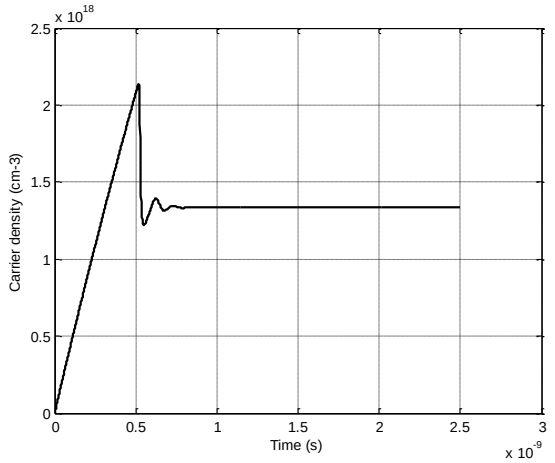

Fig. 4. Plot of carrier density vs. time for the designed 635*nm* laser for an injection current of 64 *mA*. The steady state carrier density of $1.336 \times 10^{18}\ cm^{-3}$ is found.

Using the output of the computation work above, a plot of photon density vs. time is presented in fig.5 for the designed 635*nm* red laser.

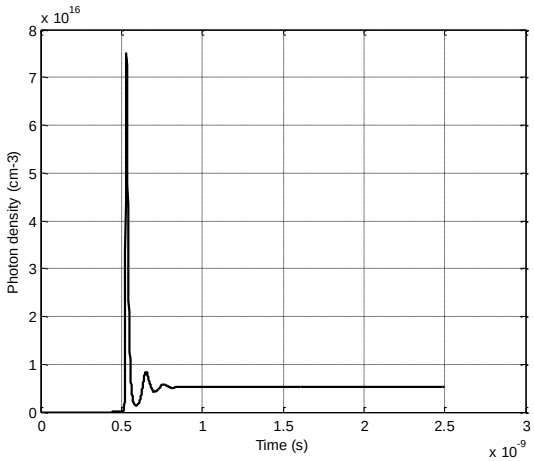

Fig. 5. Plot of photon density vs. time for the designed 635*nm* laser for an injection current of 64 *mA*. The steady state photon density of $5.283 \times 10^{15}\ cm^{-3}$ is found

From the above computations the steady state carrier density and photon density are obtained as $1.336 \times 10^{18}\ cm^{-3}$ and $5.283 \times 10^{15}\ cm^{-3}$ respectively.

The output power of the designed laser can also be expressed in terms of material gain g, mirror loss coefficient α_m, injection current I and threshold current I_{th} as [5].

$$P_o = \frac{\alpha_m h\nu \eta_i}{qg\Gamma}\ (I - I_{th}) \qquad (5)$$

where h is the Planck's constant and v is the frequency of the emitted photon.

Using the output power equation (5) and the parameter values presented above, plot of output power vs. injection current for the designed 635*nm* laser is presented in fig.6 after computations.

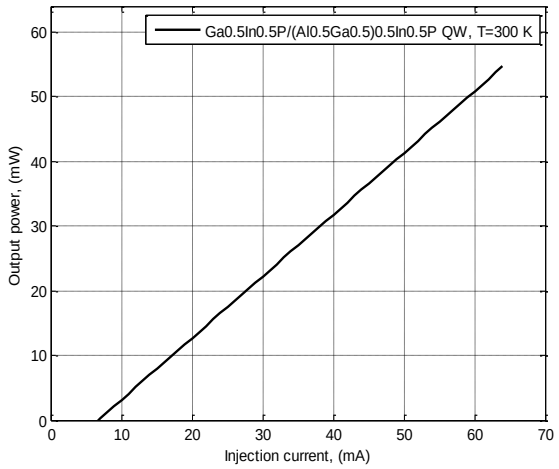

Fig. 6. Plot of output power vs. injection current for the designed 635*nm* laser.

From Fig. 6 it is found that the threshold current of the laser is 6.7 *mA* and after the threshold the output power increases with the increase of injection current.

For the designed edge emitting laser, the output power for many values of wavelength has been found out also using equation (5), where the injection current is kept constant at 64 *mA.* Using the obtained results, the plot of output power vs. wavelength is presented in Fig. 7. It is found that the material gain of the laser varies with the change in wavelength; as a result the output power of the laser also varies as equation (5). At 300K for a value of injection current of 64 *mA*, the peak intensity of output power of the designed edge emitting laser is obtained at 605.7*nm* wavelength as shown in fig.7.

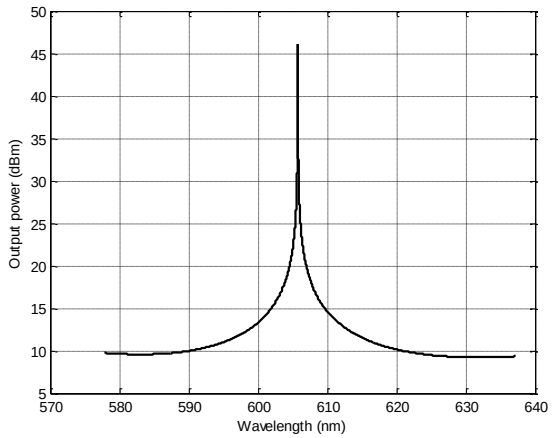

Fig. 7. Plot of output power vs. wavelength of the designed laser at 300 K, where the injection current is 64 *mA*. A peak intensity of the power is obtained at 605.7*nm* wavelength

D. Modulation Response of the designed laser

The modulation response of the designed laser has been obtained using the equation of the transfer function as given below [4-5].

$$H(f) = \frac{{f_R}^2}{{f_R}^2 - f^2 + j\frac{f}{2\pi}\gamma} \qquad (6)$$

where, f_R is the resonance frequency and γ is the damping parameter of the laser.

The above equation has been used to plot the relative response vs. frequency for a variety of injection current as shown in Fig. 8.

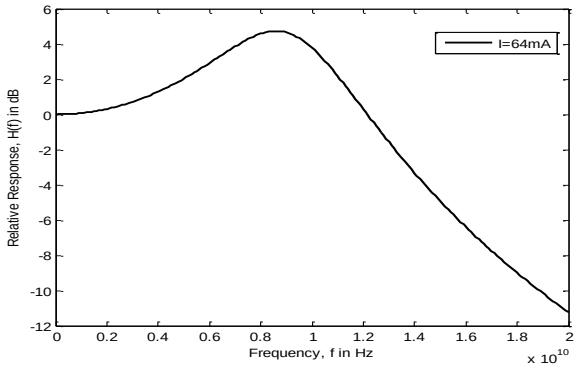

Fig. 8. Plot of relative response vs. frequency of $Ga_{0.5}In_{0.5}P/(Al_{0.5}Ga_{0.5})_{0.5}In_{0.5}P$ 80Å MQW Red Laser at 300K with an injection current of 64 *mA*.

It is found that the resonance frequency is 8.6 GHz and the modulation bandwidth is found as 13.85 GHz at 64 *mA* injection current.

V. EFFECTS OF QUANTUM WELL NUMBER VARIATION ON THE PERFORMANCE OF THE DESIGNED LASER

In this section, the effects of variation of the number of quantum well on the performance characteristics of the designed laser has been analyzed and presented. It is to be noted that the variation of the number of quantum well is achieved by keeping the volume of the cavity constant. Fig.9 and fig.10 represents the variation of carrier density and photon density with time having QW numbers of 3, 5 and 7 respectively.

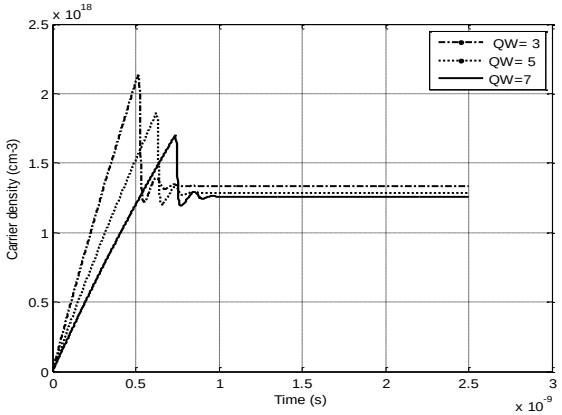

Fig. 9. Plots of carrier density vs. time for the designed 635*nm* laser for an injection current of 64 *mA* having 3QW, 5QW and 7QW respectively.

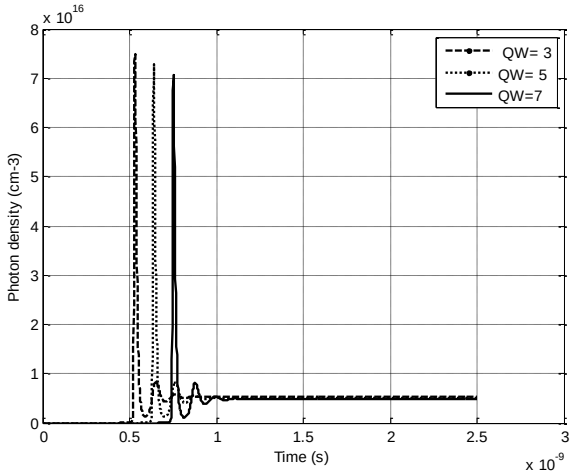

Fig. 10. Plots of photon density vs. time for the designed 635*nm* laser for an injection current of 64 *mA* having 3QW, 5QW and 7QW respectively

From Fig. 9 and fig.10 it can be found out that with the increase in the number of quantum well, there is a sharp decrement in the values of both steady state carrier density and steady state photon density.

The modal gain (i.e. confinement of material gain) of an edge emitting laser can be computed using the following equation [5].

$$\Gamma g = \Gamma g_0 \ln\left(\frac{N}{N_{tr}}\right) \qquad (7)$$

where, g_0 is the peak material gain of the active region material and N is the carrier density of the designed laser.

Fig.11 presents the variation of the modal gain with time for the laser designed with 3QW, 5QW and 7QW respectively.

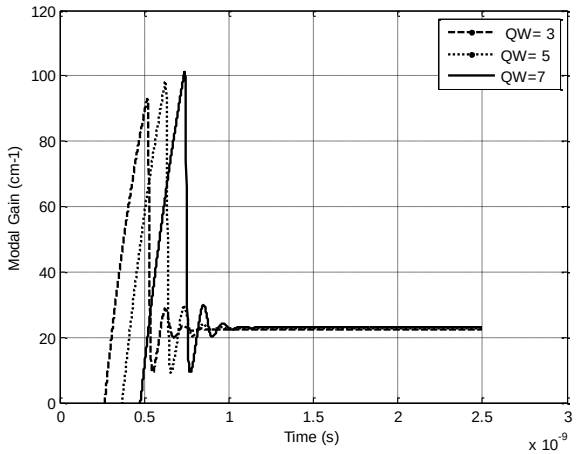

Fig. 11. Plots of modal gain vs. time of designed 635*nm* red laser having 3QW, 5QW and 7QW respectively

From the Fig. 11 it can be found that with increase in the number of quantum well, the time taken to reach steady state modal gain increases, but also with a marginal increase in the modal gain.

Fig. 12 represents the variation of output power with injection current for the designed laser having 3QW, 5QW and 7QW respectively.

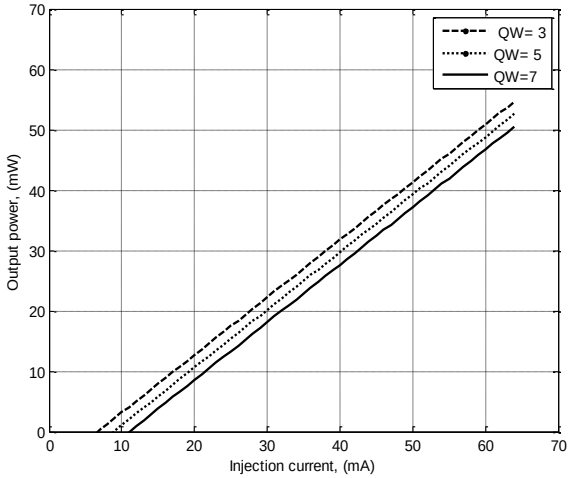

Fig. 12. Plots of output power vs. injection current for the designed 635*nm* laser having 3QW, 5QW and 7 QW respectively

It is observed that the threshold current increases with the increase of the number of QWs and as a result, the output power of the designed laser decreases.

Fig.13 represents the relative response vs. frequency plot for 3QW, 5QW and 7QW structure respectively.

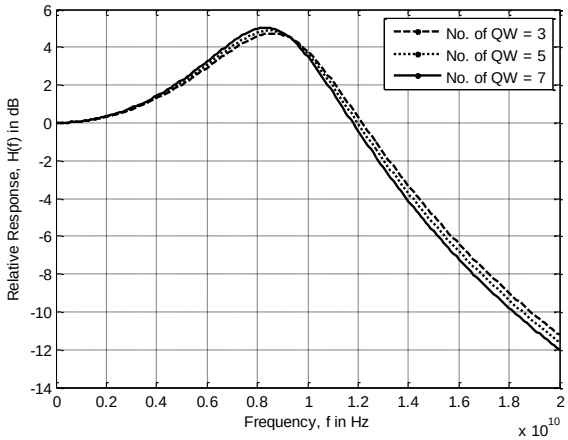

Fig. 13. Plots of relative response vs. frequency for different number of QWs of a $Ga_{0.5}In_{0.5}P/(Al_{0.5}Ga_{0.5})_{0.5}In_{0.5}P$ 80Å MQW Red Laser at 300K. A maximum resonance frequency of 8.6 GHz is obtained at 64 *mA* injection current for the designed laser having 3QWs

It is found that for a 3QW active region, a maximum resonance frequency is 8.6 GHz at 64 *mA* injection current. It is also obtained that the resonance frequency as well as the modulation bandwidth of the laser decreases with increase of the number of quantum well.

Table II contains the summarized version of simulated results of the designed laser of 3QWs structure with two other simulations conducted on the structure having 5QWs and 7QWs.

Table II. Key Results of Quantum Well Number Variation

Number of QWs	3	5	7
Confinement Factor (Γ)	0.1964	0.2679	0.3393
Threshold Current in *mA*	6.7	8.9	11.0
Steady State Modal Gain in cm^{-1}	22.41	22.79	22.99
Threshold Carrier Density in cm^{-3}	1.2902×10^{18}	1.251×10^{18}	1.2298×10^{18}
Steady State Carrier Density in cm^{-3}	1.336×10^{18}	1.286×10^{18}	1.258×10^{18}
Steady State Output Power in mW	71.18	68.47	65.76
Resonance Frequency in GHz	8.6	8.4	8.3
-3dB Bandwidth in GHz	13.85	13.6	13.4

From table II it is evident that with the increase in the number of quantum well the key performance characteristics such as the output power, resonance frequency and modulation bandwidth decreases. It has been also demonstrated that the threshold current also increases with the increase in the number of quantum well. From fig.9 and fig.10 it is evident that the turn on delay of the laser also increases with the increase in the number of quantum well.

VI. CONCLUSIONS

In this work, the dimensions of the 635*nm* MQW SCH edge emitting Red laser along with the widths of quantum wells and separate confinement heterostructure have been optimized. The MQWs have been designed with ternary compound $Ga_{0.5}In_{0.5}P$. The quantum well barriers and the SCH regions are designed with quaternary compound $(Al_{0.5}Ga_{0.5})_{0.5}In_{0.5}P$. The cladding material is also a quaternary compound $(Al_{0.7}Ga_{0.3})_{0.5}In_{0.5}P$ and the laser is based on a GaAs substrate. For the finalized dimensions, the material gain of the $Ga_{0.5}In_{0.5}P/(Al_{0.5}Ga_{0.5})_{0.5}In_{0.5}P$ MQW SCH edge emitting laser has been computed to be $766.6\,cm^{-1}$ for obtaining the performance characteristics of the laser.

At 300K the threshold current of the laser is found out to be 6.7 *mA*. A maximum steady state output power of 71.18 *mW* has been computed. A maximum steady state carrier density has been found out to be $1.336 \times 10^{18} cm^{-3}$ which is well above the threshold carrier density of $1.2902 \times 10^{18} cm^{-3}$ and transparency carrier density of $1.152 \times 10^{18} cm^{-3}$. A maximum resonance frequency of 8.6 GHz and the corresponding modulation bandwidth of 13.85 GHz at an injection current of 64 *mA* has been found for a three quantum well structure.

Furthermore the performance analysis reveals that the key performance characteristics such as the output power, resonance frequency and modulation bandwidth decreases with the increase in the number of quantum well. It has been also demonstrated that the threshold current and turn on delay also increases with the increase in the number of quantum well. As a result, the designed laser is optimized for a 3 QW active region for its better performance. The designed 635*nm* edge emitting laser is expected to perform well after fabrication. However, the design is the first of its kind designed without considering thermal degradation and some other performance parameters due to which scopes of development and improvement are still open for achieving a better performance.

REFERENCES

[1] Zh. I. Alferov "The history and future of semiconductor heterostructures", American Institute of Physics, Semiconductors, vol. 32, no. 1, pp. 1-18, 1998.

[2] Bocang Qiu, Stewart McDougall, Dan Yanson "Analysis of thermal performance of InGaP/InGaAlP quantum wells for high-power red laser diodes", NUSOD, 978-1-4244-2307-1, 2008.

[3] William T. Silvafast, *Laser Fundamentals Second Edition*, Cambridge University Press, ISBN 0-521-833450, pp. 59-61, 2004.

[4] Rinku Basak and Saiful Islam, "Performance Analysis of 980 nm $In_{0.2}Ga_{0.8}As/GaAs$ MQW VCSEL Considering Thermal Effect", The AIUB Journal of Science and Engineering (AJSE), vol. 10, no. 1, pp. 9-14, 2011.

[5] L. A. Coldren and S.W. Corzine, *Diode Lasers and Photonic Integrated Circuits*, John Wiley & Sons, Inc, pp. 1-263, 1995.

[6] I. Vurgaftman and J. R. Meyer, L. R. Ram-Mohan, "Band parameters for III–V compound semiconductors and their alloys", Journal of Applied Physics, vol. 89, no. 11, pp. 5851-5862, 2001.

[7] Weng W. Chow, Stephan W. Koch, *Semiconductor-Laser Fundamentals Physics of the Gain Materials*, ISBN 3-540-64166-1 Springer-Verlag Berlin Heidelberg New York, pp. 210-225, 1999.

[8] Sadao Adachi, *Properties of group-IV, III–V and II–VI Semiconductors*, John Wiley & Sons, ISBN 0-470-09032-4, pp. 11-359, 2005.

[9] Toby Schaer, Robert Rusnov, Stephen Eagle, Jay Jastrebski, Steven Albanese and Xavier Fernando "A Dynamic Simulation Model for Semiconductor Laser Diodes", CCECE, pp. 293-297, 2003.